International Journal on Advanced Science Engineering Information Technology

Vol.12 (2022) No. 1
ISSN: 2088-5334

Analysis of Sedimentation towards the Changes of Mangrove Area Using Multitemporal Remote Sensing Technology (A Case Study in Gresik Regency, East Java, Indonesia)

Bangun Muljo Sukojo [a,*], Nurwatik [a], Nova Nurul Annisa [a]

[a] *Department of Geomatics Engineering, Institut Teknologi Sepuluh Nopember, Surabaya, 60111, Indonesia*
Corresponding author: [*]bangunms@gmail.com

***Abstract*— Mangrove grows in coastal areas with the soil is resulted from the accumulation of mud substrate from the sedimentation process. Gresik Regency is a downstream area where the Bengawan Solo River flows, and there is the Java Sea that carries a lot of sediment material to the coast. As a result, sedimentation is forming new land increasingly that can be a place for mangroves to live. Therefore, in this study, the calculation of suspended sediment concentration and mangrove area in Gresik Regency during 2016-2019 uses Sentinel-2A satellite imagery. The purpose of these calculations is to determine the effect of sedimentation as suspended sediment on changes in the mangrove area. Mangrove area is obtained from the Maximum Likelihood supervised classification. While suspended sediment concentrations estimated from remote sensing data are obtained using four prior algorithms, they do not meet the specified accuracy requirement. This research shows that there have been changes in the mangrove area to increase and decrease during 2016-2019. The largest addition of area occurred in the period 2016-2017, which is 479.347 Ha, and the most reduction in the area occurred in the period 2018-2019, which is 534.087 Ha. The statistical test result proves that the suspended sediment as sedimentation affects the mangrove by 64.9% in the significance level of 5% or 95% confidence level.**

***Keywords*— Mangrove; sentinel-2A; suspended sediment.**

Manuscript received 21 Jun. 2020; revised 12 Dec. 2020; accepted 12 Jan. 2021. Date of publication 28 Feb. 2022.

I. INTRODUCTION

Mangroves are one of the most important ecosystems of coastal and marine areas [1]. Therefore, mangroves grow in the coastal areas in tropical and subtropical regions (30°N to 37°S) with a sedimentary environment [2]. Mangrove soils are formed by marine alluvium from the transported sediment and deposited by land, rivers, and sea [3]. Gresik Regency is a downstream area of the Solo River's mouth, the longest river in Java. This river flows from the Sewu Mountains in the southwest of Surakarta to the Java Sea.

As a result, sedimentation produces new land at the river's mouth becomes accretion [4]. Not only from the mouth of the river but also sedimentation originates from the sea, namely the Java Sea, where the currents carry sediment material to the coast. The existence of land or new land from sediment deposits can be overgrown with mangroves because the fruit that falls can be directly stuck to grow new plants [5]. From time to time, mangroves can experience changes both increase and decrease naturally, and one of them with human intervention. This change can be observed using remote sensing technology.

This study aims to determine the relationship and effect of suspended sediments on mangrove area changes in the Gresik Regency using remote sensing technology, the multitemporal Sentinel-2A satellite imagery in 2016, 2017, 2018, and 2019. This data is added with in situ data as validation data. The value of suspended sediment from image data is obtained from four prior algorithms, while the mangrove area is obtained from the classification of a land cover image using the Maximum Likelihood supervised classification method. To determine the relationship and the presence or absence of the effects of suspended sediments on the mangrove area are obtained through statistical tests using regression and hypothesis testing.

II. MATERIALS AND METHOD

This research took place in Gresik Regency, covering four districts: Ujung Pangkah District, Sidayu District, Bungah District, and Manyar District. Geographically the research

area is located between 6 ° 49'4.8 "-7 ° 8'13.2" South Latitude and 112 ° 29 '31.2 "- 112 ° 39 '57.6" East Longitude.

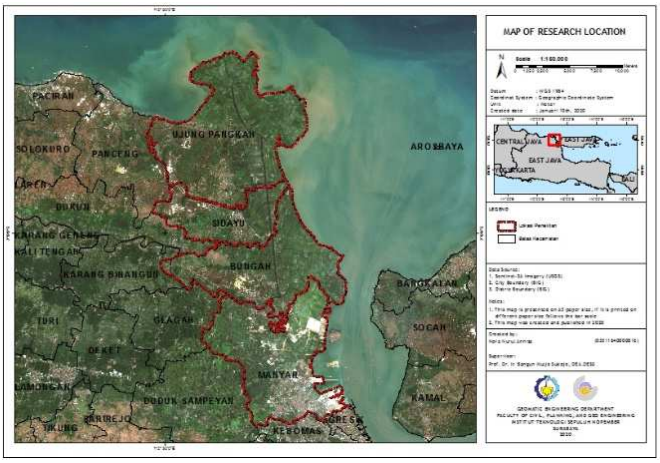

Fig. 1 Research location

A. Data and Tools

1) Data

- Sentinel-2A Level-1C satellite imagery in 2016, 2017, 2018 and 2019
- Water sample
- Sample Coordinates
- Google Earth high-resolution imagery

2) Hardware

- GPS Hand-held
- Water sampling equipment
- Water sample laboratory test equipment

3) Software

- Numerical data processing software
- Image processing software
- Spatial data processing software

B. Data Processing

1) Image Cropping: Image cropping is done to focus on the area used in the study. Moreover, it can save memory storage, and image data processing processes become faster and more effective.

2) Atmospheric Correction: Atmospheric correction for Sentinel-2A images is performed using the Sen2Cor that converts Level-1C Top of Atmospheric (TOA) Reflectance image data to Level-2A Bottom of Atmospheric (BOA) Reflectance. As needed, the resulting data is then modified from BOA reflectance to Rrs (Remote Sensing Reflectance). To convert the reflectance to Rrs uses the following equation [6].

$$Rrs(\lambda) = \frac{acr}{\pi} \quad (1)$$

where acr is atmospherical correction reflectance, in this study refers to BOA reflectance.

3) Separation of Land and Waters: Separation of land and water using the NDWI (Normalized Different Water Index) method with the aim that the land is not involved in the process of calculating suspended sediment values. Following equation [7]:

$$NDWI = \frac{(Green-NIR)}{(Green+NIR)} \quad (2)$$

where Green is the reflectance of the green band and NIR is the reflectance of the near-infrared band. NDWI value> 0 then the area is declared as land and NDWI value <0 then the area is declared as water.

4) Suspended Sediment Calculation with The Prior Algorithm: Prior algorithms that are used as follows.

- Budhiman Algorithm [8]
  Developed with case studies in the territorial waters of the Mahakam Delta, East Kalimantan, and applied to Landsat 7 and Landsat 8 imagery.
  $$TSS = 8.1429 \times exp(23.704 \times 0.95 \times red\ band) \quad (3)$$
  with $red\ band$ is the reflectance from the red band.
- Parwati Algorithm [9]
  Developed with a case study in the Berau Waters region, East Kalimantan, which was applied to Landsat 5 TM, Landsat 7 ETM, and Landsat 8 imagery.
  $$TSS = 3.3238 \times exp(34.099 \times \rho(BOA)) \quad (4)$$
  where ρ(BOA) is the Bottom of the Atmosphere reflectance of the red band.
- Jaelani Algorithm [10]
  Developed with case studies in the Poteran and Gili Iyang Waters, Sumenep, Madura, East Java, which were applied to Landsat 8. Then it was modified to be applied to Sentinel-2A with the following equation [12]:
  $$log\ (TSS) = 1.5212 \left(\frac{log\ Rrs(\lambda_2)}{log\ Rrs(\lambda_3)}\right) - 0.3698 \quad (5)$$
  where $\mathrm{Rrs}(\lambda_2)$ is the value of the reflectance remote sensing of the blue band and $\mathrm{Rrs}(\lambda_3)$ is the reflectance remote sensing of the green band in Sentinel-2A.
- Laili Algorithm (2015) [6]
  Developed with case studies in the Poteran Island Waters, Sumenep, Madura, East Java, which were applied to Landsat 8.
  $$TSS = 31.420 \left(\frac{log\ Rrs(\lambda_2)}{log\ Rrs(\lambda_4)}\right) - 12.719 \quad (6)$$
  where $\mathrm{Rrs}(\lambda_2)$ is the reflectance remote sensing of the blue band and $\mathrm{Rrs}(\lambda_4)$ is the reflectance remote sensing of the red band.

5) Choosing the Best Algorithm: The best algorithm is used to map the multitemporal suspended sediment was obtained after fulfilling the value of the requirement for R^2 (corresponding value/determination coefficient), NMAE (Normalized Mean Absolute Error), and RMSE (Root Mean Square Error). R^2 must meet the requirement of >70% [11]. The NMAE has requirement value of ≤ 30% [12] and for RMSE, the closer it gets to zero is the better. The equation that is used are as follows [13].

$$NMAE\ (\%) = \frac{1}{N}\sum_{i=1}^{N}\left|\frac{x_{estimated,i}-x_{measured,i}}{x_{measured}}\right| \times 100\% \quad (7)$$

$$RMSE = \sqrt{\frac{\sum_{i=1}^{N}(x_{estimated,i}-x_{measured,i})^2}{N}} \quad (8)$$

where N is the amount of data, $x_{estimated,i}$ is the estimated value of suspended sediment (the processing result), and

$x_{measured,i}$ is the value of the measurement result (as a value that is considered correct).

6) Reclassify: Reclassify is done to change the processing results of suspended sediment concentrations to be divided into certain classes so that the distribution is visible. The concentration class is divided into seven classes that 0-5 mg/l, 5-15 mg/l, 15-50 mg/l, 50-100 mg/l, 100-150 mg/l, 150-220 mg/l, dan >220 mg/l.

7) Color Composite: Color composite is used to identify the mangrove area. The composite that is used for Sentinel-2A is RGB 8,11,4 (NIR, SWIR, Red). It will sharpen the visualization and because the mangrove should be in dark red. The dark red caused by tidal effects on inertidal area that create distinctive character of soil types and that affects the vegetation community reflectance [14].

8) Supervised Classification: Supervised classification is used to get the area covered by mangrove vegetation. The classification method used is in this supervised classification is the Maximum Likelihood classification. The Maximum Likelihood method will classify each pixel into a class that has the highest probability of belonging [15]. This process results are the data in vector format, especially the mangrove vector, which will be used to calculate the mangrove area.

9) Confusion Matrix Accuracy Test: The accuracy of the classification results is calculated by using the confusion matrix method. The accuracy obtained from this matrix includes the producer's accuracy (pa_i), user's accuracy (ua_i), overall accuracy (O^c), and kappa coefficient ($\widehat{K}$). Here is the equation for calculating this accuracy [16], [17].

$$pa = X_{ii}/X_{+i} \quad (9)$$

$$pa = X_{ii}/X_{i+} \quad (10)$$

$$O^c = \frac{\sum_{i=1}^{r} Xii}{N} \times 100\% \quad (11)$$

$$\widehat{K} = \frac{N\sum_{i=1}^{r} Xii - \sum_{i=1}^{r}(X_{i+}\, X_{+i})}{N^2 - \sum_{i=1}^{r}(X_{i+}\, X_{+i})} \quad (12)$$

Description:

N : The total number of samples
X_{i+} : the marginal totals of row i
X_{+i} : The marginal totals of column i
Xii : The number of observations in row I and column i

10) Calculation of Mangrove and Suspended Sediment Area: Calculation of suspended sediment area and mangrove area using the overlay method with analysis tools available in the spatial data processing software.

11) Correlation and Hypothesis Testing: This is the final stage, namely the correlation testing used for knowing the strength and direction of the relationship of the mangrove area variable and the suspended sediment area variable using linear correlation. Correlation condition that is considered correct if r value is -1 < r <1. Besides, the hypothesis test uses a t-test as a significance test to determine whether sedimentation with the suspended sediment area variable affects the change of mangrove with the mangrove area variable.

III. Results and Discussion

A. Calculation of Suspended Sediment Concentration with the Prior Algorithms

The concentration of suspended sediment from image data to be processed using the four prior algorithms was obtained from Sentinel-2A image processing with the acquisition date of December 25, 2019, then compared with in situ data at 10 observation points has been taken on the same date as the image data. In situ data is shown in Table I.

TABLE I
SUSPENDED SEDIMENT CONCENTRATION FROM IN SITU

Point	Coordinates (m)		Suspended Sediment Concentration In Situ (mg/l)
	Easting (X)	Northing (Y)	
1	669,005	9,241,471	124
2	668,898	9,241,707	60
3	669,176	9,241,314	84
4	667,771	9,240,333	146
5	667,537	9,240,302	328
6	666,663	9,240,434	256
7	667,309	9,240,341	276
8	666,333	9,240,504	284
9	666,681	9,240,360	292
10	668,048	9,240,367	182

The calculation result of suspended sediment concentration using the four prior algorithms, namely the Budhiman Algorithm, Parwati Algorithm, Laili Algorithm, and Jaelani Algorithm, is shown in Table II.

TABLE II
SUSPENDED SEDIMENT CONCENTRATION FROM THE PRIOR ALGORITHM

Point	Suspended sediment concentration (mg/l)			
	Jaelani	Laili	Parwati	Budhiman
1	19.791	20.831	656.192	320.944
2	20.433	20.759	1,980.810	691.786
3	20.051	20.852	1,825.161	653.529
4	19.917	21.854	3,106.860	945.930
5	19.996	22.151	3,838.288	1,095,683
6	19.902	22.023	9,314.764	2,029.283
7	20.744	22.633	5,547.214	1,415.357
8	18.685	21.117	14,810.660	2,801.225
9	19.788	22.186	8,295.087	1,872.152
10	18.808	21.451	1,740.077	632.197

Table II shows that there is a significant difference in the results of suspended sediment concentration from image data to in situ data. Changes in current and wind can cause this difference, and the algorithm has local properties which are suitable for the place and time where the algorithm was made. Therefore, it is not necessarily appropriate to be applied to waters with different characteristics and different retrieval times.

B. Validation for the Prior Algorithm

Validation is obtained from the correlation value, RMSE (Root Mean Square Error), and NMAE (Normalized Mean Absolute Error). Here is a linear regression graph for the accuracy of the algorithm shown in Figure 2.

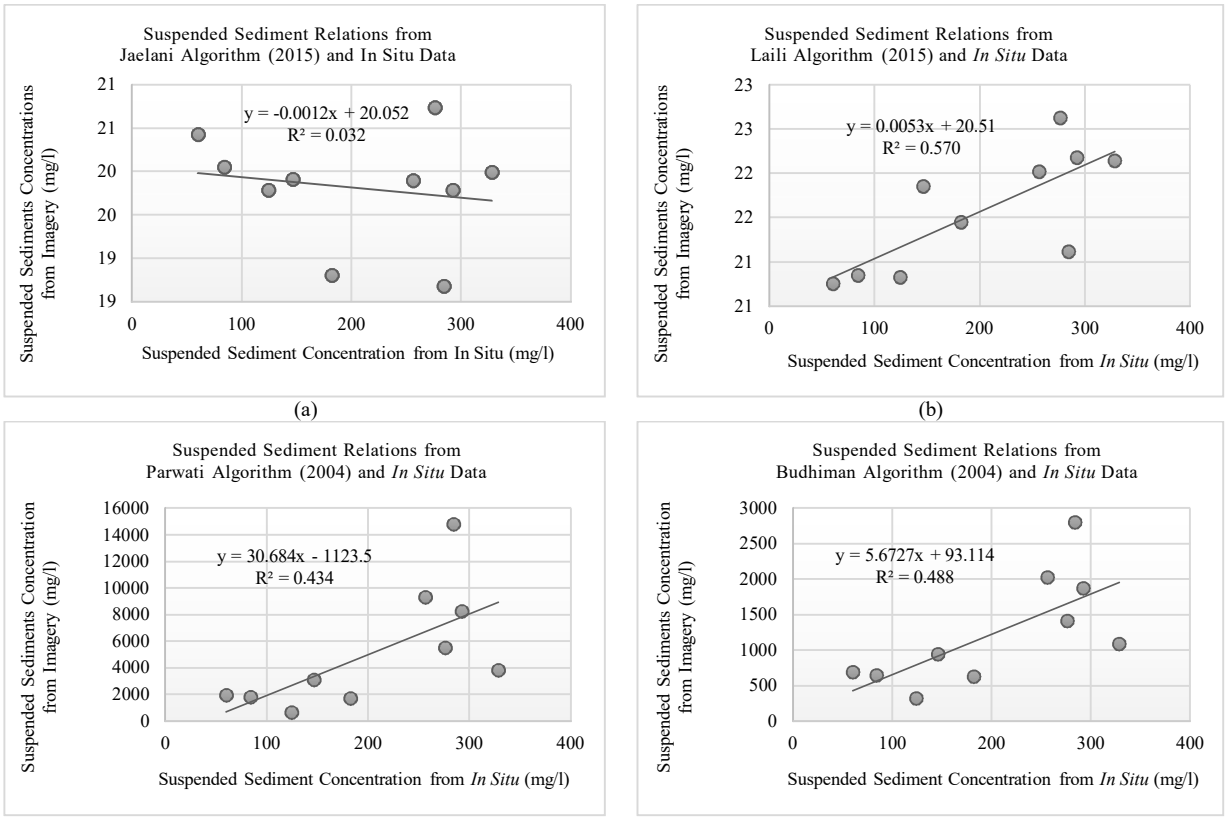

Fig. 2 Linier regression graph of suspended sediment processing result of the four algorithms within situ data. (a) Jaelani Algorithm, (b) Laili Algorithm, (c) Parwati Algorithm, and (d) Budhiman Algorithm

TABLE III
VALIDATION TEST RESULT FOR THE PREVIOUS ALGORITHM

No.	Algorithm	R^2	NMAE (%)	RMSE (mg/l)
1	Jaelani	0.032	86.740	204.768
2	Laili	0.570	85.843	202.916
3	Parwati	0.434	2,296.190	6,445.470
4	Budhiman	0.487	558.234	1,280.480

Based on these values in Table III, the four prior algorithms do not meet the NMAE value's suitability requirements, with their RMSE value is very high. The NMAE value that does not meet these requirements is not in line with the determination coefficient's value. The best algorithm is one that meets the NMAE compatibility requirements with the lowest RMSE value and has a strong relationship within situ data. Therefore, a new equation is needed to estimate the concentration of suspended sediment from image data.

C. Development of A New Equation Model

The new equation model is made by using mathematical approaches using regression between the concentration data of suspended solids in the field with the satellite image reflectance values obtained from the single-band, the ratio of two-band, or inter-band chromatization. The regression will be applied to visible light waves namely red band (0.646-0.685 nm), blue band (0.493-0.535 nm), and green band (0.537-0.582 nm). The regression model equation uses exponential functions to avoid negative values and extreme values.

TABLE IV
DETERMINATION COEFFICIENT OF FOR SINGLE BAND

Single-Band	Equation	R^2
B2	$y = 22.834 \times e^{12.913x}$	0.208
B3	$y = 18.937 \times e^{10.874x}$	0.181
B4	$y = 9.0949 \times e^{14.546x}$	0.476

TABLE V
DETERMINATION COEFFICIENT OF FOR TWO BAND

Two-Band	Equation	R^2
B2/B3	$y = 0.055 \times e^{10.587x}$	0.152
B2/B4	$y = 47.5817 \times e^{-10.12x}$	0.051
B3/B2	$y = 72.0276 \times e^{-6.396x}$	0.152
B3/B4	$y = 3.000.000 \times e^{-9.686x}$	0.818
B4/B2	$y = 0.0732 \times e^{6.0631x}$	0.492
B4/B3	$y = 0.007 \times e^{-10.237x}$	0.813

TABLE VI
DETERMINATION COEFFICIENT OF FOR INTER-BAND CROMATIZATION

Inter-Band Chromatization	Equation	R^2
(B2/(B2+B3+B4))	$y = 3{,}000{,}000 \times e^{-34.71x}$	0.151
(B3/(B2+B3+B4))	$y = 3 \times 10^{12} \times e^{-6..75x}$	0.812
(B4/(B2+B3+B4))	$y = 5 \times 10^{-5} \times e^{42.41x}$	0.714

Based on Table IV-IV, the best regression model belongs to the ratio of the green and red bands (B3/B4) with a coefficient of determination of 0.818. This shows that the

reflectance ratio results have a strong relationship to the suspended sediment data in situ. The mathematical equation resulting from this modeling using Sentinel-2A image data is as follows.

$$\text{TSS} = 3{,}000{,}000 \times exp\left(-34.71 \times \left(\frac{BOA\ reflectance\ of\ B3}{BOA\ reflectance\ of\ B4}\right)\right) \quad (13)$$

where TSS is total suspended solid or suspended sediment concentration in mg/l, B3 is the green band, and B4 is the red band. Then the equation is applied to the image with the acquisition date of December 25, 2019 and compared with *in situ* data shows the results as Table VII and the regression can be seen in Fig. 3.

TABLE VII
COMPARISON BETWEEN THE RESULTS OF MATHEMATICAL EQUATION WITHIN SITU DATA

Points	Suspended Sediment Concentrations (mg/l)	
	Mathematical Equation	*In Situ*
1	85.867	124
2	66.808	60
3	83.039	84
4	199.034	146
5	241.801	328
6	224.996	256
7	267.868	276
8	175.720	284
9	262.759	292
10	218.143	182

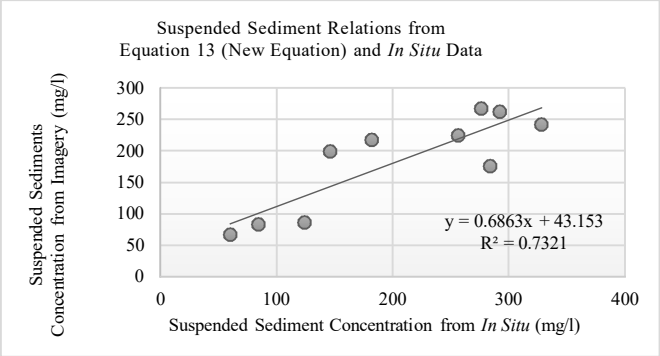

Fig. 3 Linear regression graph of suspended sediment from Equation 13 result and In Situ

Equation 13 has fulfilled the suitability requirements for NMAE, RMSE, and R^2 with the respective values of 18.890%, 51.632 mg/l, and 0,732. This shows that the new algorithm can be used for further processing in multitemporal images.

D. Distribution and Changes in Area of Suspended Sediments

The distribution of suspended sediment concentrations in the territorial waters of the Gresik Regency in 2016-2019 was obtained from image processing using Equation 13. Here are the results showed in Fig. 4.

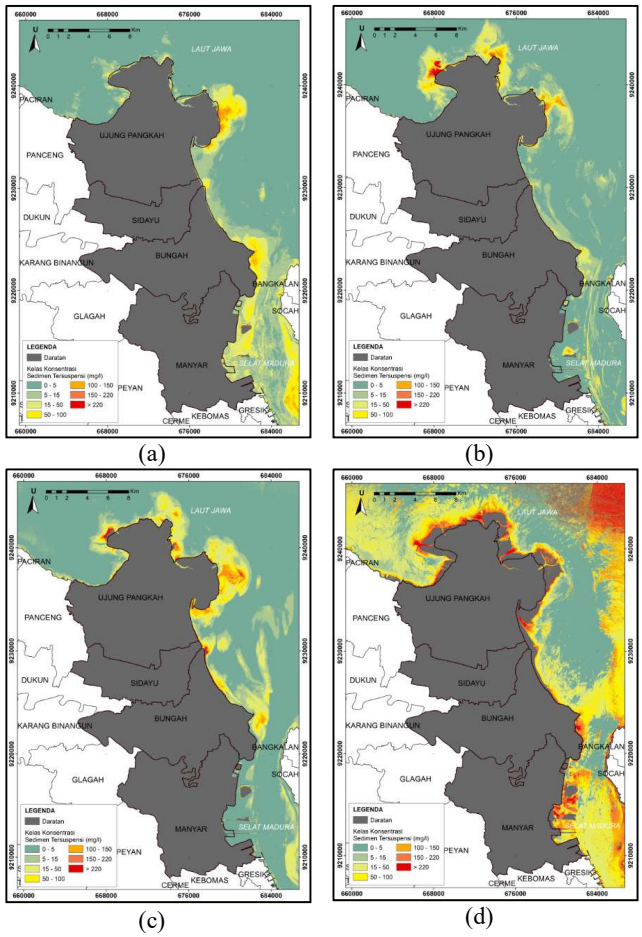

Fig. 4 The distribution of suspended sediment concentration annually (a) 2016, (b) 2017, (c) 2018, dan (d) 2019

TABLE VIII
THE AREA OF SUSPENDED SEDIMENT IN 2016

No.	Class (mg/l)	Area (Ha)	Percentage (%)
1	0-5	7,866.754	47.186
2	5-15	4,993.619	29.953
3	15-50	2,603.338	15.615
4	50-100	961.826	5.769
5	100-150	218.412	1.310
6	150-220	27.663	0.166
7	> 220	0.069	0.000
	Total	16,671.681	100.000

TABLE IX
THE AREA OF SUSPENDED SEDIMENT IN 2017

No.	Class (mg/l)	Area (Ha)	Percentage (%)
1	0-5	9,408.524	57.241
2	5-15	3,877.547	23.591
3	15-50	2,047.954	12.460
4	50-100	661.753	4.026
5	100-150	250.875	1.526
6	150-220	109.373	0.665
7	> 220	80.751	0.491
	Total	16,436.777	100.000

TABLE X
THE AREA OF SUSPENDED SEDIMENT IN 2018

No.	Class (mg/l)	Area (Ha)	Percentage (%)
1	0-5	9,134.759	56.646
2	5-15	2,381.522	14.768
3	15-50	2,758.139	17.104
4	50-100	1,152.983	7.150
5	100-150	468.106	2.903
6	150-220	168.436	1.045
7	> 220	62.032	0.385
	Total	16,125.977	100.000

TABLE XI
THE AREA OF SUSPENDED SEDIMENT IN 2019

No.	Class (mg/l)	Area (Ha)	Percentage (%)
1	0-5	2,764.650	20.547
2	5-15	1,707.082	12.687
3	15-50	4,114.455	30.579
4	50-100	2,420.384	17.989
5	100-150	1,087.362	8.081
6	150-220	911.674	6.776
7	> 220	449.439	3.340
	Total	13,455.046	100.000

Based on Table VIII-XI, it is known that there is a decrease in the area of suspended sediment concentration each year. The highest decrease occurred in the period 2018-2019 with an area of 2,670.931 Ha, and the least occurred in the period 2016-2017 with an area of 234.904 Ha. The average decrease in each period is 1,072.212 Ha.

The existence of this decline proves that there has been an increase in land area in the Gresik Regency or a linear reduction in the size of the water area as one of the effects of increased sedimentation. The changes in the suspended sediment area in 2016-2019 if it is made in graphical form, results are shown in Fig. 5.

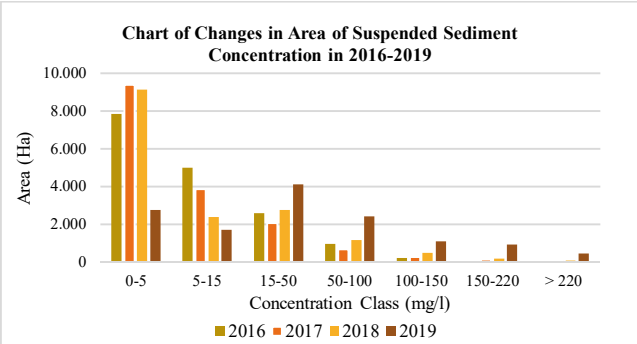

Fig. 5 Graph of the area of suspended sediment concentration in 2016-2019

E. *Mangrove Identification*

The identification of mangrove vegetation uses RGB 8,11,4 color composites (NIR, SWIR, Red). From the results of the color composite, the mangrove looks brick red or brownish red. The color contrasts with the surrounding objects such as ponds that are purplish-blue, orange for non-mangrove vegetation, and green for settlements. The classification results are shown in Fig. 6.

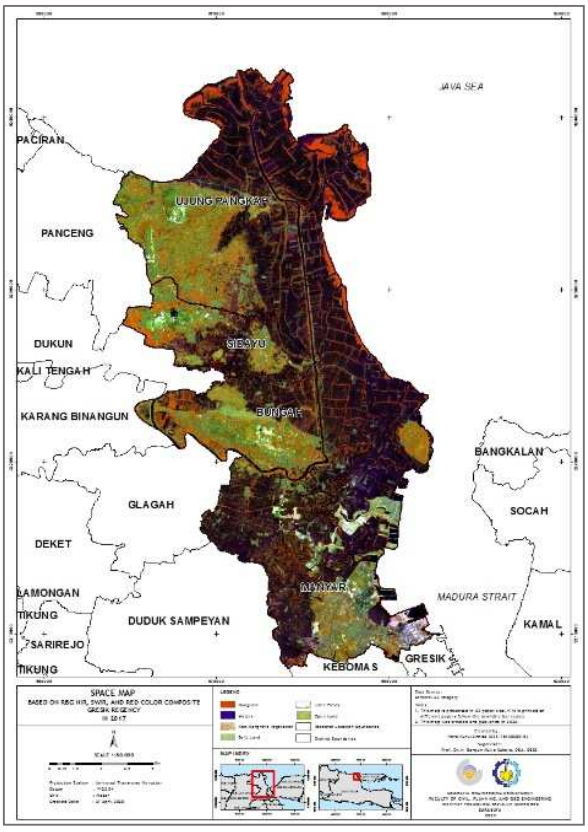

Fig. 6 RGB 8,11,4 color composites on Sentinel-2A images in 2017

F. *Accuracy of Classification Result*

Accuracy test results of land cover classification to get mangrove vegetation is using the confusion matrix method. The accuracy requirement uses the overall accuracy criterion of ≥80%. This accuracy test is applied to the image of the results of the guided classification of Maximum Likelihood with the acquisition date of November 5, 2019. The reference data to find out the real object is a high-resolution image obtained from Google Earth.

TABLE XII
CONFUSION MATRIX FROM LAND COVER CLASSIFICATION RESULT

Class	1	2	3	4	5	Total	UA
1	43	0	7	0	0	50	86
2	4	37	4	2	3	50	74
3	0	3	47	0	0	50	94
4	0	1	12	37	0	50	74
5	0	0	10	1	39	50	78
Total	47	41	80	40	42	250	
PA	91.489	90.244	58.750	92.500	92.857		

Class description:
Class 1 = Mangrove
Class 2 = Non-mangrove vegetation
Class 3 = Land built
Class 4 = Open land
Class 5 = Waters

Based on Table XII, the overall accuracy for land cover classification is 81.2%, and the kappa coefficient is 0.765. This shows that the processing results have met the criteria set by ≥ 80%. The kappa coefficient is good according to the following interpretation of the kappa coefficient [12].

< 0.2 = Poor
0.21 - 0.40 = Fair
0.41 - 0.60 = Moderate
0.61 - 0.80 = Good
> 0.80 = Very Good

G. Distribution and Changes in Mangrove Area

From the results of the supervised classification of Sentinel-2A images, the distribution of mangroves at the study site in 2016-2019 is obtained in Fig. 7.

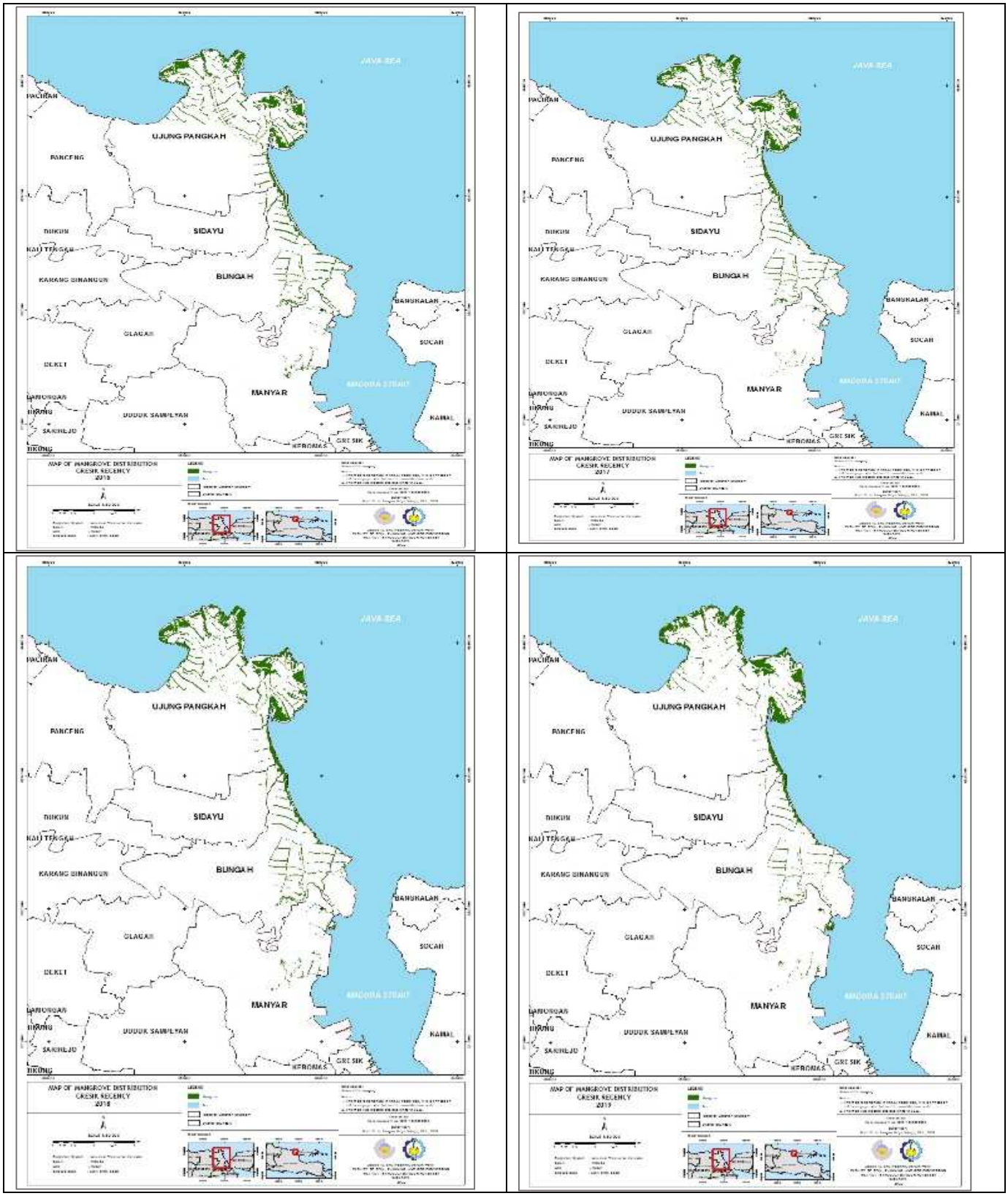

Fig. 7 The distribution of mangrove annually (a) 2016, (b) 2017, (c) 2018, dan (d) 2019

TABLE XIII
MANGROVE AREA IN 2016-2019

No.	District	Area (Ha)			
		2016	2017	2018	2019
1	Bungah	865.559	425.743	479.419	293.230
2	Manyar	353.917	84.564	126.961	73.510
3	Sidayu	84.810	89.670	100.280	84.810
4	Ujung Pangkah	1,196.994	1,349.749	1,399.323	1,205.052
	Total	2,501.280	1,949.730	2,105.980	1,656.602

Mangroves at the study site are unevenly distributed. It can be seen that Ujung Pangkah District has the largest mangrove area compared to the other three districts. Mangroves in Ujung Pangkah District are scattered on the north and east coast and around the pond area. For Sidayu District, Bungah District, and Manyar District, mangroves spread on the east coast and around the pond area. The amount of change that is decreasing and increasing the area of mangrove forests from year to year is presented in the graph in Fig. 8.

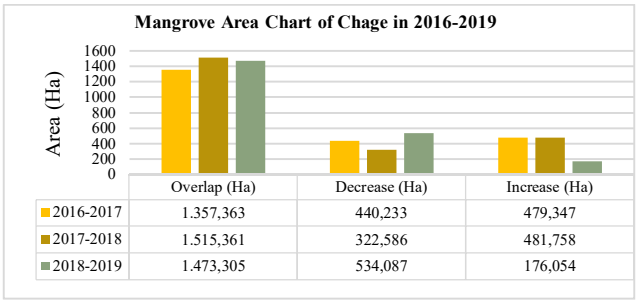

Fig. 8 Mangrove area chart of the change in 2016-2019

Changes that occur during the four years are explained as follows.

- From 2016 to 2017, there was a change in the form of mangrove areas which increased more than those that decreased. Mangrove forests area increased by 479.347 hectares and decreased by 440.233 hectares. The overlapping area is 1,357.363 hectares.
- From 2017 to 2018, there was a change in the form of mangrove areas which increased more than those that decreased. Mangrove forests area is increased by 481.758 hectares and decreased by 322.586 hectares. The overlapping area is 1,515.361 hectares.
- From 2018 to 2019, there was a change in mangrove areas which decreased more than those increased. Mangrove forests area is increased by 176.054 hectares and decreased by 534.087 hectares. The overlapping area is 1,473.305 hectares.

It can be seen that the average decrease and increase in a period is 432.302 hectares and 379.053 hectares. The reduction of mangrove areas in Gresik Regency, namely in the Ujung Pangkah District, Sidayu District, and Bungah District, can occur because of mangrove areas' conversion into pond areas for aquaculture. Meanwhile, in Manyar Subdistrict, most of the damage was caused by converting mangroves into industrial and aquaculture areas. Simultaneously, the increase in mangrove areas is caused by mangroves that grow naturally in the soil as a result of the accumulation of sedimentation and human intervention with reforestation.

H. Effect of Suspended Sediment on Mangrove

The effect of sedimentation from suspended sediment data on mangrove area changes is known by calculating correlation using linear regression and significant testing using a t-test. The following is the correlation result is showed in Fig. 9.

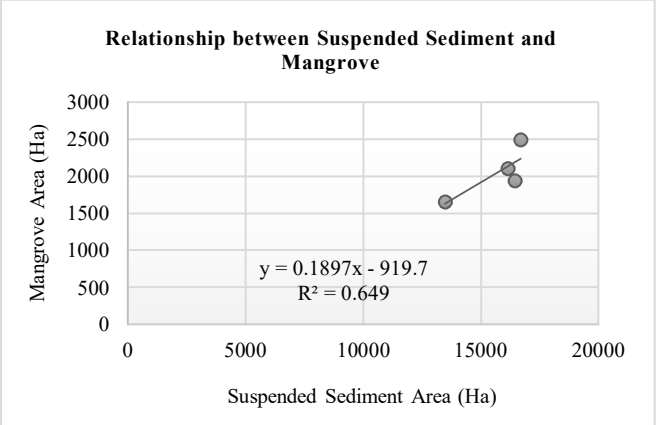

Fig. 9 Graph of the relationship of suspended sediments on mangroves

The form of the linear equation from the correlation results above is y = 0.1897x - 919.7. It shows a positive correlation (directly proportional) which means that if the area of suspended sediment increases, the area of mangrove will also increase, and vice versa if the area of suspended sediment decreases, the area of mangrove will also decrease.

The calculation result gets the determination coefficient (R^2) of 0.649, which means that the suspended sediment variable affects mangroves by 64.9%, and the remaining 35.1% is affected by other variables besides the variables which are used in this study. At the same time, the strength of the relationship between the two variables is expressed by the correlation coefficient (r). The correlation coefficient value is 0.806. The correlation coefficient is interpreted according to the following statement below [18].

0.00 - 0.20 = Very low
0.21 - 0.40 = Low
0.41 - 0.60 = Medium
0.61 – 0.80 = Strong
0.81 – 1.00 = Very strong

Based on the results of the correlation coefficient and interpretation according to the statement above, it can be seen that the suspended sediment and mangrove has a strong relationship. Then hypothesis testing is performed using the t-test with the tested hypothesis are:

- Ho: There is no significant effect between suspended sediment and mangrove area
- Ha: There is a significant effect between suspended sediment on mangrove area

Decision-making on the results of hypothesis testing uses a significance level (α) of 0.05 or 5%, which is the same as a confidence level of 95%. The criteria for this test are as follows:

- If –t table < t count < t table, then Ho is accepted, and Ha is rejected.
- If –t table > t count > t table, then Ho is rejected, and Ha is accepted.

From the test result, the value of t count was 17.737. With a degree of freedom (df) of 6 in the 0.05 degree of significance, the value of t table was 2.450. This shows that t count > t table so that Ho is rejected, and Ha is accepted. So, the result of this test states that suspended sediment as part of sedimentation has a significant effect on changes in mangrove area in Gresik Regency with a significance level of 5% or a 95% confidence level.

IV. CONCLUSIONS

Based on the result and explanation above, this research can be concluded that suspended sediment concentrations in Gresik Regency Waters estimating by four prior algorithms do not meet the specified accuracy requirement. So, the new equation from mathematical approaches is used to estimate those concentrations. Based on statistical test result, this research also proved that the suspended sediment as sedimentation and mangrove has a strong relationship by r value of 0.806. The sedimentation affected the mangrove by 64.9% in the significance level of 5% or 95% confidence level.

ACKNOWLEDGMENT

We are grateful to ITS Directorate of Research and Community Service for funding this work by program ITS Laboratory Research Local Funding 2020 with contract number: 894/PKS/ITS/2020.

REFERENCES

[1] S. P. Sari and D. Rosalina, "Mapping and Monitoring of Mangrove Density Changes on tin Mining Area," *Procedia Environ. Sci.*, vol. 33, pp. 436–442, 2016.

[2] I. C. Feller, C. E. Lovelock, U. Berger, K. L. McKee, S. B. Joye, and M. C. Ball, "Biocomplexity in mangrove ecosystems," *Ann. Rev. Mar. Sci.*, vol. 2, no. 1, pp. 395–417, 2010.

[3] M. D. Hossain and A. A. Nuruddin, "Review Article Soil and Mangrove : A Review," *J. Environ. Sci. Technol.*, vol. 9, no. 2, pp. 198–207, 2016.

[4] A. L. Rakhmawati, "Sustainable Coastal Protection in Pasuruan City : Jetty Structure in Rejoso Estuary Sustainable Coastal Protection in Pasuruan City : Jetty Structure in Rejoso Estuary," in *IOP Conference Series: Earth and Environmental Science*, 2019.

[5] N. Anggraini, M. Hartuti, and S. Marpaung, "Pemantauan Distribusi Sedimentasi di Ujung Pangkah Kabupaten Gresik Menggunakan Data Landsat," in *Seminar Nasional Penginderaan Jauh*, 2015, pp. 575–584.

[6] N. Laili *et al.*, "development of water quality parameter retrieval algorithms for estimating total suspended solids and chlorophyll-a concentration using landsat-8 imagery at poteran island water," *ISPRS Ann. Photogramm. Remote Sens. Spat. Inf. Sci.*, vol. 2, no. 2W2, pp. 55–62, 2015.

[7] W. Li *et al.*, "A comparison of land surface water mapping using the normalized difference water index from TM, ETM+ and ALI," *Remote Sens.*, vol. 5, no. 11, pp. 5530–5549, 2013.

[8] S. Budhiman, T. W. Hobma, and Z. Vekerdy, "Remote sensing for Mapping TSM concentration in Mahakam Delta: an analytical approach," *13th Omi. Work. Valid. Appl. Satell. Data Mar. Resour. Conserv.*, no. January, pp. 5-1-5–14, 2004.

[9] L. Indeswari, T. Hariyanto, and C. B. Pribadi, "Pemetaan Sebaran Total Suspended Solid (TSS) Menggunakan Citra Landsat Multitemporal dan Data In Situ (Studi Kasus : Perairan Muara Sungai Porong, Sidoarjo," *J. Tek. ITS*, vol. 7, no. 1, pp. C71–C72, 2018.

[10] L. M. Jaelani and R. Y. Ratnaningsih, "Spatial and temporal analysis of water quality parameter using sentinel-2A data; Case study: Lake Matano and Towuti," *Int. J. Adv. Sci. Eng. Inf. Technol.*, vol. 8, no. 2, pp. 547–553, 2018.

[11] T. Hariyanto, T. C. Krisna, C. B. Pribadi, A. Kurniawan, B. M. Sukojo, and M. Taufik, "Evaluation of Total Suspended Sediment (TSS) Distribution Using ASTER, ALOS, SPOT-4 Satellite Imagery in 2005-2012," *IOP Conf. Ser. Earth Environ. Sci.*, vol. 98, no. 1, 2017.

[12] L. M. Jaelani, R. Limehuwey, N. Kurniadin, A. Pamungkas, E. S. Koenhardono, and A. Sulisetyono, "Estimation of Total Suspended Sediment and Chlorophyll-A Concentration from Landsat 8-Oli: The Effect of Atmospher and Retrieval Algorithm," *IPTEK J. Technol. Sci.*, vol. 27, no. 1, 2016.

[13] L. M. Jaelani, B. Matsushita, W. Yang, and T. Fukushima, "An improved atmospheric correction algorithm for applying MERIS data to very turbid inland waters," *Int. J. Appl. Earth Obs. Geoinf.*, vol. 39, pp. 128–141, 2015.

[14] G. Winarso and A. D. Purwanto, "Evaluation of Mangrove Damage Level Based on Landsat 8 Image," *Int. J. Remote Sens. Earth Sci.*, vol. 11, no. 2, p. 105, 2017.

[15] J. R. Otukei and T. Blaschke, "Land cover change assessment using decision trees, support vector machines and maximum likelihood classification algorithms," *Int. J. Appl. Earth Obs. Geoinf.*, vol. 12, no. Suppl. 1, pp. 27–31, 2010.

[16] C. Liu, P. Frazier, and L. Kumar, "Comparative assessment of the measures of thematic classification accuracy," *Remote Sens. Environ.*, vol. 107, no. 4, pp. 606–616, 2007.

[17] F. Nkomeje, "Comparative Performance of Multi-Source Reference Data to Assess the Accuracy of Classified Remotely Sensed Imagery: Example of Landsat 8 OLI Across Kigali City-Rwanda," *Int. J. Eng. Work. Kambohwell Publ. Enterp.*, vol. 4, no. 1, pp. 10–20, 2015.

[18] S. Rauf, M. M. Pasra, and Yuliani, "Analysis of correlation between urban heat islands (UHI) with land-use using sentinel 2 time-series image in Makassar city," *IOP Conf. Ser. Earth Environ. Sci.*, vol. 419, no. 1, 2020.